Raman Spectroscopic and Visible Absorption Investigation of $LiCrSi_2O_6$ Pyroxene Under Pressure

C. J. S. POMMIER,* G. J. REDHAMMER, M. B. DENTON, and R. T. DOWNS

Pharmaceutical Research Institute, Bristol-Myers Squibb, PO Box 191, New Brunswick, New Jersey 08903-0191 (C.J.S.P.); Department of Materials Engineering, Division of Mineralogy, University of Salzburg, Hellbrunnerstr. 34, A-5020 Salzburg, Austria (G.J.R.); Department of Chemistry, University of Arizona, Tucson, Arizona 85721-0041 (M.B.D.); and Department of Geosciences, University of Arizona, Tucson, Arizona 85721-0077 (R.T.D.)

The first observation of the vibrational spectrum of the synthetic pyroxene Li-kosmochlor ($LiCrSi_2O_6$) is reported herein. The Raman and visible spectra are reported as a function of pressure. Though the pyroxene retains its $P2_1/c$ symmetry, changes in the Raman spectra are observed between 6.8 and 7.7 GPa, possibly due to the formation of an additional bond between Li and O3 or some other transition that retains the mineral's $P2_1/c$ space group. Splitting of the peak appearing at approximately 700 cm^{-1}, used to characterize the $P2_1/c$ phase in other studies, is not observed. Comparison is made with the Raman spectra of $LiAlSi_2O_6$ and $LiFeSi_2O_6$ in the $P2_1/c$ phase and the visible spectra of $NaCrSi_2O_6$ at high pressures.

Index Headings: **High-pressure Raman spectroscopy; Pyroxene; Pressure-induced phase change; Visible spectroscopy.**

INTRODUCTION

Lithium-kosmochlor, $LiCrSi_2O_6$, is a monoclinic, optically biaxial synthetic member of the pyroxene group of minerals. Pyroxenes (general formula $M2M1Si_2O_6$) comprise approximately 25% of the Earth's volume to a depth of 400 km.[1] There are a variety of symmetries exhibited by pyroxenes, most notably *C2/c*, $P2_1/c$, *Pbca*, and *Pbcn*, and most pyroxenes appear to undergo phase transitions between these various symmetries as a function of pressure and temperature. Low temperatures often induce the same or similar phase transitions as high pressures because both are associated with a decrease in cell volume. The atomic scale mechanisms for these changes have been the subject of much study.[2] A recently discovered phase transition in Mg–Fe rich pyroxenes, accompanied by a volume change, is now accepted as an origin of deep-focus earthquakes whose origins cluster at a depth of about 225 km.[3–5]

In $LiCrSi_2O_6$, single chains of CrO_6 (M1) octahedra are parallel to single chains of SiO_4 tetrahedra (Fig. 1). Li occupies the M2 site. In general, in pyroxenes the M2 site is observed to be 4-, 5-, 6-, or 8-coordinated, depending on pressure, temperature, and composition of the pyroxene. In *C2/c* symmetry there are three symmetrically nonequivalent oxygens, designated as O1, O2, and O3. O1 oxygens are at the apices of the SiO_4 tetrahedra. O2 are on the base of the tetrahedra, and O3 are on the base of the tetrahedra bridging the silicon atoms.

Recently, a detailed structural analysis of $LiMe^{3+}Si_2O_6$ has been performed utilizing X-ray crystallography, where Me^{3+} = Al, Ga, Cr, V, Fe, Sc, and In.[6] The temperature-dependent phase transition of $LiCrSi_2O_6$ has been examined with X-ray crystallography along with the other synthetic pyroxenes named above.[7] At room temperature and pressure, Li-kosmochlor ($LiCrSi_2O_6$) displays space group symmetry of $P2_1/c$, but above 330 K it is in *C2/c* symmetry.[6,7] Spodumene ($LiAlSi_2O_6$) and $LiCrSi_2O_6$ behave similarly at the phase transition; both go from 6- to 5-coordination of the Li atom. Therefore, the study of $LiCrSi_2O_6$ at room temperature is analogous to the study of $LiAlSi_2O_6$ above its phase transition at 3.2 GPa and is also similar to the study of $LiFeSi_2O_6$ at temperatures below its phase transition at 229 K or at pressures above 1 GPa, where it is also 5-coordinated around the Li atom.[7,8] This study will compare the Raman spectra of $LiCrSi_2O_6$, $LiFeSi_2O_6$, and $LiAlSi_2O_6$ in the $P2_1/c$ phase.

By factor-group analysis, there should be 30 Raman-active A_g modes and 30 Raman-active B_g modes when $LiCrSi_2O_6$ is in the $P2_1/c$ phase. While the *C2/c* phase of $LiCrSi_2O_6$ is not studied in this paper, it is interesting to note that in the *C2/c* phase, both Li and Cr occupy positions of C2 site symmetries, and the Si and three types of oxygens display C1 site symmetry. The coordination change from *C2/c* to $P2_1/c$ destroys the C2 symmetry displayed by the M cations, such

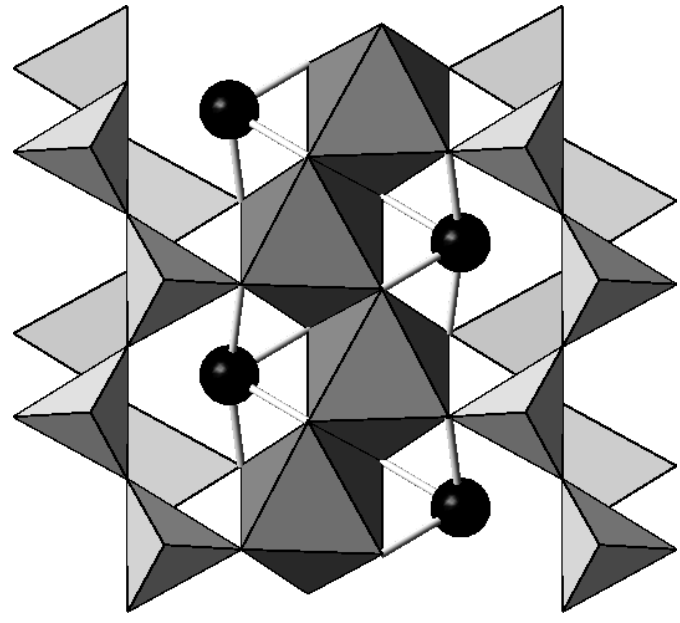

FIG. 1. Structure of $LiCrSi_2O_6$ in *C2/c* phase, as viewed down a. SiO_4 chains are shown as linked tetrahedrons, one chain pointing toward the viewer and another pointing away. Li atoms are shown as spheres with their 4-fold coordination in *C2/c* phase represented. CrO_6 chains are presented as polyhedrons.

Received 8 November 2007; accepted 24 April 2008.

* Author to whom correspondence should be sent. E-mail: carolyn.pommier@bms.com.

0003-7028/08/6207-0766$2.00/0

TABLE I. Ruby R1 and R2 fluorescent peak shifts and calculated pressures for the visible absorption experiment.[a]

Shift $R1_p$–$R1_s$ (± 7 cm^{-1})	Calculated pressure R1 (± 0.9 GPa)	Shift $R2_p$–$R2_s$ (± 6 cm^{-1})	Calculated pressure R2 (± 0.7 GPa)
68	9.1	79	10.7
75	10.1	82	11.0
60	8.0	70	9.4
68	9.1	73	9.9
67	9.0	73	9.8
47	6.3	57	7.6
49	6.5	57	7.6
46	6.2	54	7.3
45	5.9	53	7.0
44	5.9	51	6.9
43	5.7	50	6.8
35	4.6	42	5.6
34	4.6	41	5.5
11	1.4	14	1.9
12	1.6	16	2.1
1	0.1	3	0.4
0	0.0	2	0.3

[a] Ruby fluorescence measurements were made before and after collection of the visible spectrum. The pressure reported is the pressure after the collection of the spectrum.

that in the $P2_1/c$ phase, all atoms occupy sites with C1 symmetry.

The purpose of this paper is to investigate the pressure-induced changes in the Raman spectra of $LiCrSi_2O_6$ and the accompanying changes in the visible spectra and to draw analogies to bonding changes observed in previous work.[9,10] To date, there has been no report of the vibrational spectra of $LiCrSi_2O_6$. Study of $LiCrSi_2O_6$ under pressure will increase the body of knowledge pertaining to the mechanism of the phase transitions in the Li-pyroxenes, which will lead to better understanding of the phase transitions of pyroxenes.

EXPERIMENTAL

Synthesis. The sample, a dark green single crystal fragment of dimensions 100 μm × 65 μm × 30 μm, was synthesized by Günther Redhammer as detailed in a previous publication.[6]

High-Pressure Raman Spectroscopy. A 4-pin Merrill Basset type diamond anvil cell (DAC) with 600 μm culets was utilized to apply pressure to the sample. A stainless steel gasket was preindented to 60 μm and a 320 μm hole was electrostatically drilled in the indentation to form the cell chamber. The cell was loaded with the above-mentioned fragment in an undetermined orientation. Because the specimen was a single crystal, it is possible that there is some dependence of the intensity of the Raman bands on the orientation of the crystal. No special care was taken to enhance or to minimize the potential polarization effects. Each Raman spectrum was collected with the sample in the same orientation, so while the absolute intensities of the Raman modes may be affected by the orientation of the crystal, the relative intensities between the collections should be representative of the changes due to pressure.

A small chip of ruby and the 4:1 methanol:ethanol pressure medium were also included in the cell. The crystal occupied approximately 4% of the volume of the 0.005 μL cell. Utilizing an 1800 grooves/mm grating centered at 529.5 nm, the region from 85 cm^{-1} to 998 cm^{-1} was acquired using WinSpec software. The region from 404 cm^{-1} to 1279 cm^{-1} was acquired with the spectrometer centered at 538 nm and a calibration offset of 564.5 nm. Raman scattering was collected in the backscattered geometry through a Mitutoyo MPlan 10× objective with a 1.32 in. working distance and 0.28 numerical aperture (NA). A spatial filter was utilized to minimize signal contribution from diamonds or other material surrounding the sample. Rayleigh scattering was filtered out using two Kaiser Optics holographic notch filters. Spectra were acquired using a Jobin Yvon Spex HR 460 spectrometer and a liquid nitrogen cooled 1152 × 256 pixel Princeton Instruments charge-coupled device (CCD) held at approximately −100 °C.

In general, the error in pressure below 10 GPa measured with the ruby scale is about 0.05 GPa. In this study the error may be slightly higher (~0.1 GPa) because the ruby became lodged into gasket contact. We have accounted for the non-hydrostatic pressures around the ruby chip as well as possible, and the reported pressures were the reading after the Raman spectrum was acquired because there is typically significant relaxation after a pressure change. Ruby fluorescence and Raman spectra were excited with a 514.5 nm Ar^+ laser.

Pressure applied to the $LiCrSi_2O_6$ crystal was hydrostatic via the pressure medium—the sample was not under deviatoric stress—so the Raman spectra were not affected by deviatoric stresses as the ruby emissions were.

To establish that the chromium in the sample did not interfere with the chromium fluorescence from the ruby that was utilized for the pressure measurement, the $LiCrSi_2O_6$ crystal was removed from the sample chamber and examined separately from the ruby. In the spectroscopic region where ruby fluoresces there was no Cr^{3+} emission from the pyroxene sample observed, so there was no interference with the ruby fluorescence pressure measurement from the sample.

Ten Raman spectra were collected at ten different pressures. One spectrum was collected with the sample in air (not in a DAC). Nine spectra were acquired as the pressure in the sample was increased from 2.3 GPa to 9.9 GPa in a DAC. At 9.9 GPa, the crystal was inspected under a microscope and it was found that the crystal had changed color and small crystals of the pressure medium were beginning to form. Any additional increase in pressure would have further solidified the pressure medium and the stress applied to the sample would have been deviatoric instead of hydrostatic. No photograph of the color change was acquired.

Visible Absorption Spectroscopy. After collection of Raman data, the cell was removed from the sample holder and examined under an optical microscope. It was observed that the crystal had changed from a deep green to a purplish-red color. Visible absorption spectroscopy was utilized to characterize this change. As pressure was released, absorption spectra were collected through the diamond anvil cell utilizing 200 μm diameter fiber optics coupled to an SI-Photonics 440 series ultraviolet–visible (UV-Vis) spectrophotometer. The SMA ends of the fibers were butted against the diamond windows

TABLE II. Raman shifts of peaks with increasing pressure (in cm^{-1}).[a]

Pressure (Gpa)	In air	2.3	4.7	5.2	5.4	6.1	6.8	7.7	8.0	8.3	8.8	9.9
Peak 1	114.5	114.7	114.5	114.4	115.3	115.2	114.9	114.7	114.7	114.9	115.5	114.3
Peak 2		121.0		122.8	125.1	126.9	129.9	128.9	133.9		138.2	139.0
Peak 3			139.2		137.9			146.7				
Peak 4			155.4		156.4	159.6	158.0	158.3	157.9	158.5	160.1	159.4
Peak 5	154.1	161.9	165.2	165.3		170.2		171.7	173.9	177.0	179.2	180.0
Peak 6											200.9	201.6
Peak 7	181.0	189.8	191.7	191.9	195.1	195.2	196.2	198.6	201.1	204.9		209.5
Peak 8	192.9	198.9	201.6	201.5	204.6	205.3	206.3	209.2	212.1	216.9		223.0
Peak 9	226.9	229.2	230.3	229.9	232.2	232.2	232.7	234.3	236.2	239.3	241.5	242.9
Peak 10	259.6	265.9	267.7	268.3	270.5	271.1	273.1	276.1	279.8	285.8	282.8	283.9
Peak 11	287.1	283.2	283.9	284.6	286.4	286.7	287.8	288.1	292.0	297.8	292.1	295.4
Peak 12	298.8	296.2	297.3	298.2	296.5		301.5	304.8	306.8	312.1	318.4	
Peak 13									328.2	331.9	333.1	
Peak 14	323.6	336.1	338.0	338.4	341.1	342.0	344.1	348.1	347.6	351.5	353.0	355.0
Peak 15									358.0		363.6	369.5
Peak 16					355.2					367.8	377.1	373.8
Peak 17		357.0	361.8	359.2	365.5			366.3	373.3	384.6	391.1	384.7
Peak 18	375.8	379.8	383.8	382.2	384.1			387.6	394.1	403.6	401.8	405.2
Peak 19	406.9	409.4	411.3	411.3	414.0	414.0	416.3	418.0	420.7	423.9	422.7	428.5
Peak 20	415.7	420.1	422.5	423.2	426.5	427.0	430.1	434.9	440.2	448.8	455.8	462.2
Peak 21		444.6	446.2	447.3	449.8	451.0	454.0	458.8	464.2	472.9	481.0	486.9
Peak 22			495.8	497.2	498.8	498.4	500.0	502.0	505.3	511.3	517.8	521.1
Peak 23		518.6	518.0	517.3	520.0	519.5	520.0	522.3	525.0	529.5	533.3	536.0
Peak 24	518.5	524.7	526.5	527.0	529.3	530.0	531.6	534.4	537.8	542.6	548.3	550.8
Peak 25	536.1	545.7	547.9	548.2	549.7	551.4	553	566.6	560.8	567.7	573.6	578.7
Peak 26	556.4	561.0	563.2	562.8	562.9	566.0	566.3	570.2	573.9	580.7	586.1	591.3
Peak 27	576.1	589.5	593.0	594.3	597.5	598.8	601.9	607.3	612.7	621.3	628.8	634.9
Peak 28							681.4	683.7	688.2	693.2	698.4	704.4
Peak 29	686.0	690.3	692.2	692.9	695.7	696.7	698.7	703.0	708.0	715.6	722.1	727.2
Peak 30	776.2	784.9	786.1	788.9				793.9	797.4	800.7	809.1	
Peak 31								806.7	812.6	819.2		816.8
Peak 32		850.8	850.1	850.7		853.9						
Peak 33	854.0	861.0	863.4	864.9				869.8	866.7	874.2	882.2	888.3
Peak 34		881.4	884.0	884.1	885.5	887.0	888.9	894.0	898.9	904.3	910.3	916.2
Peak 35	929.0	931.6	934.2	935.0	938.0	939.2	942.4	948.2	954.3	964.5	972.9	982.1
Peak 36							978.5	981.7	987.5	987.6	986.4	
Peak 37	998.0	995.9	998.4	999.1	1001.5	1002.7	1005.7	1010.6	1015.3	1020.6		
Peak 38	1015.8	1026.4	1028.6	1029.4	1031.2	1032.5	1035.5	1041.1	1044.4	1048	1052.2	1056.7
Peak 39	1049.5	1054.6	1057.4	1059.0	1061.5			1072.9	1078.4	1090.7	1100.2	1107.2
Peak 40	1090.3	1081.0	1077.4	1075.3	1072.9	1069.3	1066.2	1062.9	1062.0			
Peak 41		1098.5	1098.9	1098.9	1100.0	1100.0	1101.8	1105.7	1109.5	1116.4	1122.0	1125.6

[a] Peak 1 does not appear to be a Raman mode, as it does not shift with pressure. The error in shift measurement is estimated to be 0.5 cm^{-1}. Peaks 1–3 were not included in the analysis as they are instrumental artifacts.

to allow for maximum light throughput. Light was introduced into the spectrometer through a 50 μm × 400 μm slit. Using a 325.5 grooves/mm grating blazed at 300 nm, the range collected was from 400 nm to 950 nm. The detector was a linear CCD array with 3700 pixels with dimensions of 8 μm × 200 μm. The same calibration curve generated for the calibration of pressure for the Raman spectra was used to find the pressures of the sample inside the cell for the visible absorption spectra (Table I).

RESULTS AND DISCUSSION

High-Pressure Raman Spectroscopy. As the sample was already in $P2_1/c$ symmetry, no discontinuous phase changes were expected; however, some changes in the Raman spectra were observed. These changes were consistent with the observed spectra of other pyroxenes at pressures above their phase transitions.[9,10] As with the $P2_1/c$ pyroxenes discussed in previous work,[9] $LiCrSi_2O_6$ should have 60 Raman peaks associated with it, 30 A_g modes and 30 B_g modes. Only 43 peaks are observed. (Table II) The spectra are similar to the spectra of $LiFeSi_2O_6$ and $LiAlSi_2O_6$ in the $P2_1/c$ phase (Fig. 2). As the materials are so similar in nature, i.e., they are all pyroxenes with different substitutions of a single metal ion, the similarity in spectra is not surprising. The factor group analysis is identical, with the force constants and polarizabilities of bonds changing due to the change in chemistry of the material. This similarity suggests several important generalizations about Li-pyroxenes. First, the $P2_1/c$ phase of Li-pyroxenes appears to display a characteristic set of modes below 600 cm^{-1}: a singlet near 170 cm^{-1}, which in this work is labeled ν_4; a doublet near 200 cm^{-1} (ν_6 and ν_7); a singlet at 250 cm^{-1} or below (ν_8); two low-intensity peaks (ν_{10} and ν_{11}) at lower frequencies than two high-intensity doublets (ν_{12}, ν_{13}, ν_{18}, ν_{20}); a singlet near 450 cm^{-1} (ν_{21}); a low-intensity singlet, (ν_{22}); a doublet (ν_{24} and ν_{25}) between 450 cm^{-1} and 550 cm^{-1}; and finally, a high-intensity doublet (ν_{26} and ν_{27}) near 550 cm^{-1}. The doublet observed in $LiCrSi_2O_6$ near 200 cm^{-1} (ν_6 and ν_7) corresponds to the spodumene peak labeled ν_3 in previous work,[9] which split at the $C2/c$ to $P2_1/c$ phase transition and was associated to an Si–O3–Li vibration. In spodumene, the ν_3 portion of the doublet is not observable at high pressures (>3.5 GPa) and in this experiment, the intensity of ν_6 decreases dramatically at high pressures, which suggests that ν_6 of $LiCrSi_2O_6$ and ν_3 of

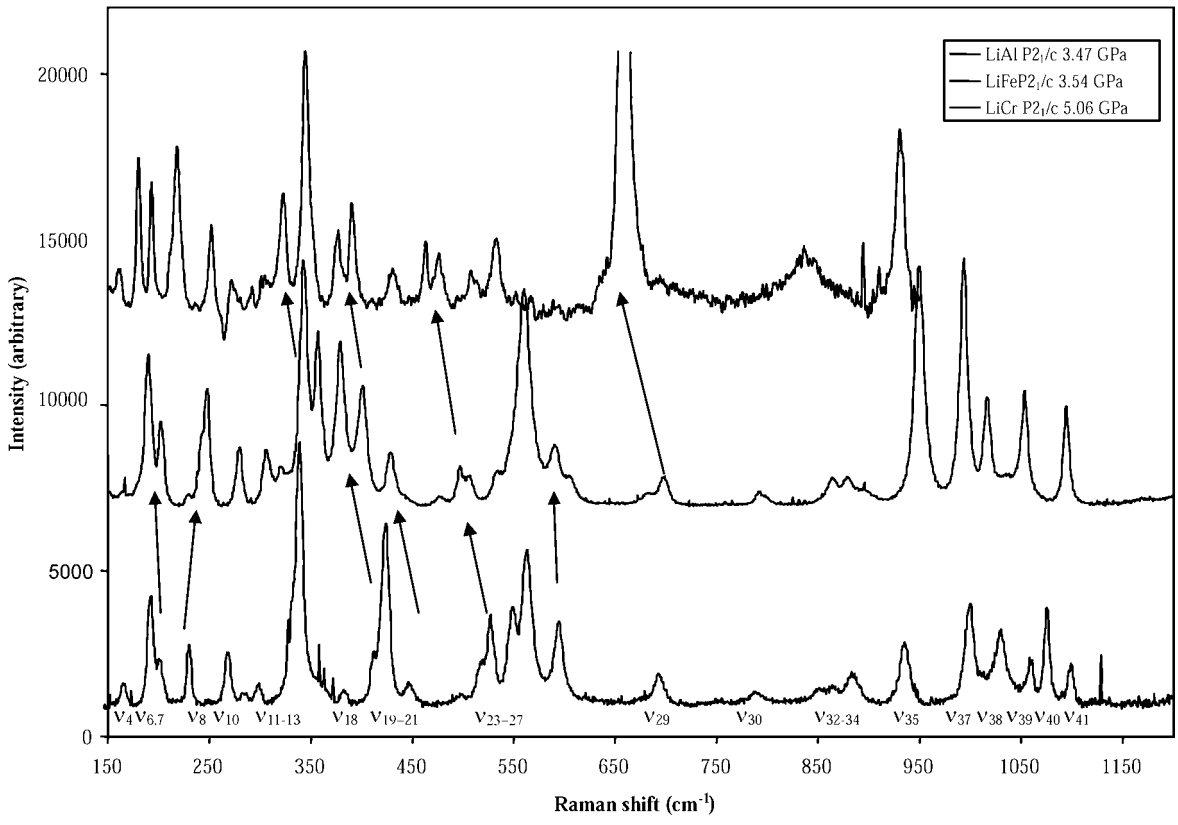

FIG. 2. Plots of three Li-pyroxenes in the $P2_1/c$ phase. These plots display the similarity of the Raman spectra of the three Li-pyroxenes studied herein. Assignments of Raman modes can be made by comparison of the Raman spectra of both $LiFeSi_2O_6$ and $LiCrSi_2O_6$, though more studies must be performed to confirm the mode assignments.

$LiAlSi_2O_6$ may be similarly assigned. The singlet at 250 cm^{-1} (ν_8) appears to be the same mode (assigned as ν_5 in previous work)[9] that appears in spodumene at the phase transition. If this is the same mode, it is expected that this peak would not be apparent in the Raman spectra of the $C2/c$ phase of $LiCrSi_2O_6$. One of the two low-intensity peaks (ν_{10} and ν_{11}) corresponds to the mode labeled ν_{10} in spodumene, which appeared at the phase transition of $LiAlSi_2O_6$, so it is expected that this peak should also not be apparent in the $C2/c$ spectrum of $LiCrSi_2O_6$, though that phase is not reported in this work.[9] The high-intensity doublet (ν_{12}, ν_{13}) appears to be similar to modes ν_{11} and ν_{14} of spodumene,[9] which were assigned to Si–O2 vibrations that was coupled to Si–O3 vibrations. The second doublet (ν_{18}, ν_{20}) corresponds to the spodumene modes labeled as ν_{16} and ν_{17},[9] which were associated with an Si–O3 stretch. The singlet near 450 cm^{-1} (ν_{21}) appears to be similar to ν_{18} in spodumene, which appeared at the phase transition.[9] Finally, the doublet near 550 cm^{-1} (ν_{26} and ν_{27}) appears to correspond to peaks assigned as ν_{19} and ν_{20} in spodumene.[9]

In $LiCrSi_2O_6$, many of the doublets have one high-intensity peak and one low-intensity peak (e.g., the doublet near 350 cm^{-1} looks more like a singlet with a shoulder). This phenomenon could be because the $LiCrSi_2O_6$ spectrum shown in Fig. 2 was acquired at a higher pressure than the $LiAlSi_2O_6$ or $LiFeSi_2O_6$. Intensity changes are observed with changes in pressure (Fig. 3). Also, note that in general, the peaks in $LiCrSi_2O_6$ appear at a higher wavenumber than the peaks in $LiFeSi_2O_6$, which, in turn, appear at higher wavenumbers than the peaks for $LiAlSi_2O_6$. This may be due to a number of reasons, including different pressures at which the spectra were acquired, different electronegativity of the M1 atom, and different ionic radius of the M1 atoms. Modes at higher frequencies indicate more energetic vibrations, so the bonds in $LiCrSi_2O_6$ are of higher energy than the bonds in $LiFeSi_2O_6$ or $LiAlSi_2O_6$ under the pressures plotted in Fig. 2.

Figure 3 presents the Raman spectra of $LiCrSi_2O_6$ as pressure is increased. Other than the expected shifting of peaks with pressure that accompanies the increase in bond energy associated with decrease of cell volume (Fig. 4), there is little change in the Raman spectrum of $LiCrSi_2O_6$ under pressure until 7.6 GPa. At this pressure, several changes in the Raman spectra are observed, which may be indicative of a phase change.

First, a peak near 692 cm^{-1} appears, forming a doublet. Previously, Si–O3 stretching has been assigned to this region. As this sample is $P2_1/c$ throughout all pressures studied, if this band were Si–O3 stretching, there should have been two separate modes throughout all pressures, one for each symmetrically nonequivalent Si–O3 chain. The doublet in this investigation is not related to the $P2_1/c$ symmetry, which lends evidence to previous assertions that the use of the mode near 700 cm^{-1} as an indicator of $P2_1/c$ symmetry is a poor choice for the Li-pyroxenes.[9,10]

Second, at 7.6 GPa several interesting Raman peak intensity

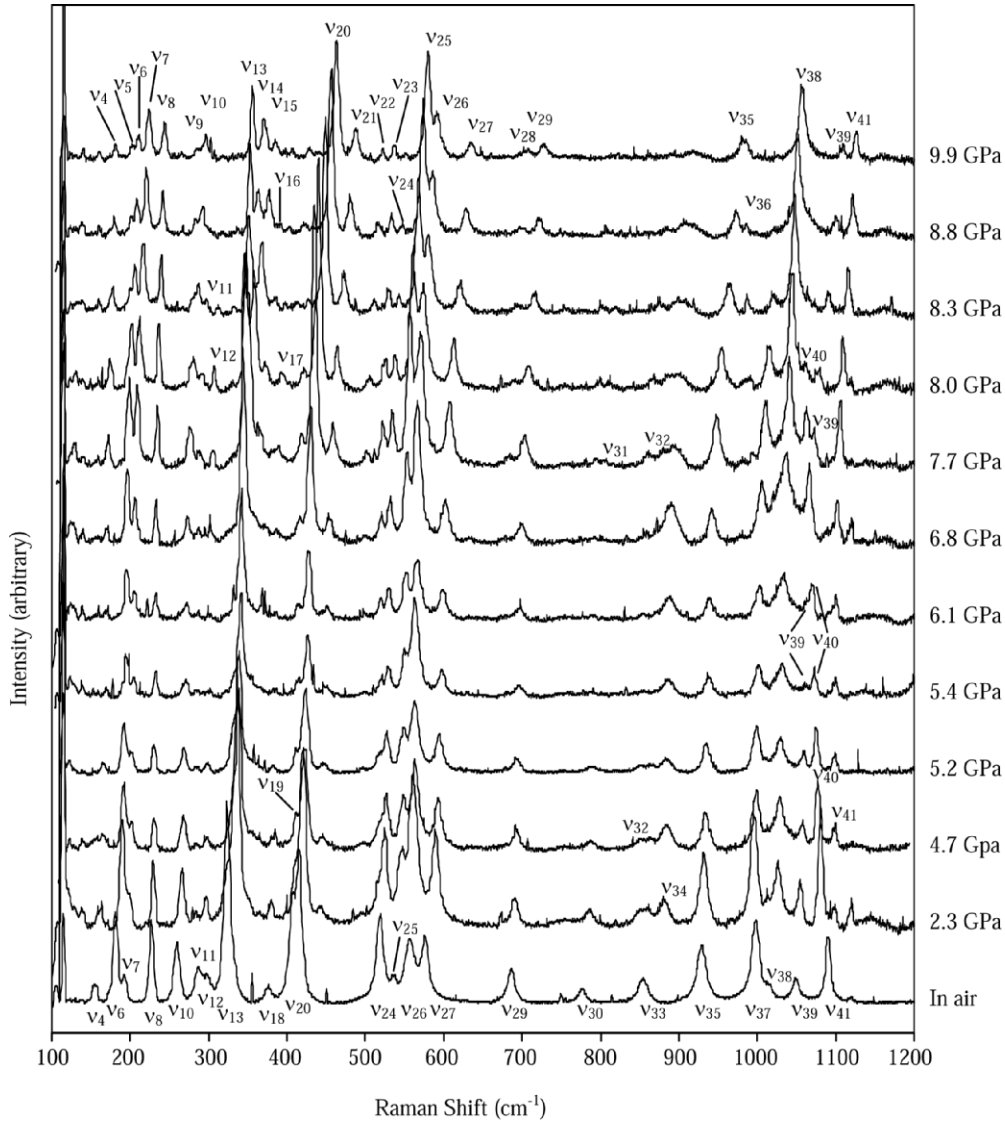

FIG. 3. Raman spectra of $LiCrSi_2O_6$ as pressure is increased. The material is already in $P2_1/c$ phase, so no additional phase transformation is expected. However, changes in the Raman spectra are observed near 5.2 GPa and near 8.8 GPa. This is the first presentation of the vibrational spectra of this material.

changes occur. The mode at 1010 cm^{-1} begins to decrease significantly in intensity, eventually disappearing entirely from the spectrum by 9.9 GPa. The relative intensities of the peaks at 551 cm^{-1} and 574 cm^{-1} invert. The previously weak 551 cm^{-1} band becomes more intense than the 564 cm^{-1} band. In addition, a mode at 375 cm^{-1}, which was previously only a shoulder of the peak at 349 cm^{-1}, becomes more intense and the singlet at 348 cm^{-1} becomes a doublet at 346 cm^{-1} and 349 cm^{-1}. Finally, the soft mode—the mode that decreases in Raman shift from 1090 cm^{-1} to 1062 cm^{-1} as pressure is increased—goes to zero intensity above 7.6 GPa.

In addition to the intensity changes at 7.6 GPa, the slope of the change in Raman shift with pressure increases for most of the Raman peaks above this pressure. These changes in the derivative of Raman shift of $LiCrSi_2O_6$ with pressure occur near the same pressure region (approximately 8 GPa) where changes occur in the Raman spectra of the other two Li-pyroxenes examined previously.[9,10] The changes are consistent with a coordination change of the Li atom from 5 to 6. This coordination change would retain the $P2_1/c$ symmetry.

Visible Absorption Spectroscopy. Color change has been previously noted in pyroxenes and other minerals.[11,12] For instance, $LiAlSi_2O_6$ pyroxene is a valued gemstone because it is strongly pleochroic, i.e., its color changes with orientation. Neither kosmochlor, $NaCrSi_2O_6$,[13] nor Li-kosmochlor, $LiCrSi_2O_6$, displayed a phase change within the pressure realm studied. Kosmochlor remained in $C2/c$ symmetry due to the presence of the large cation, Na, in the M2 site, while Li-kosmochlor remained in $P2_1/c$ symmetry. At temperatures above 329 K, $LiCrSi_2O_6$ is in $C2/c$ phase,[7] so studying the material at room temperatures is similar to studying other clinopyroxenes at high pressures if one makes the argument that similar phase transitions are brought about by decreased temperature as are observed by increased pressure. Kosmochlor progresses from emerald-green to greenish-blue with increasing pressure. Previous studies of other materials have shown a discontinuous change in color with the change in bond structure.[12] Kosmochlor displays no such discontinuity. Likewise, as the color of the $LiCrSi_2O_6$ progresses from a deep emerald-green to a reddish-purple, no discontinuity is

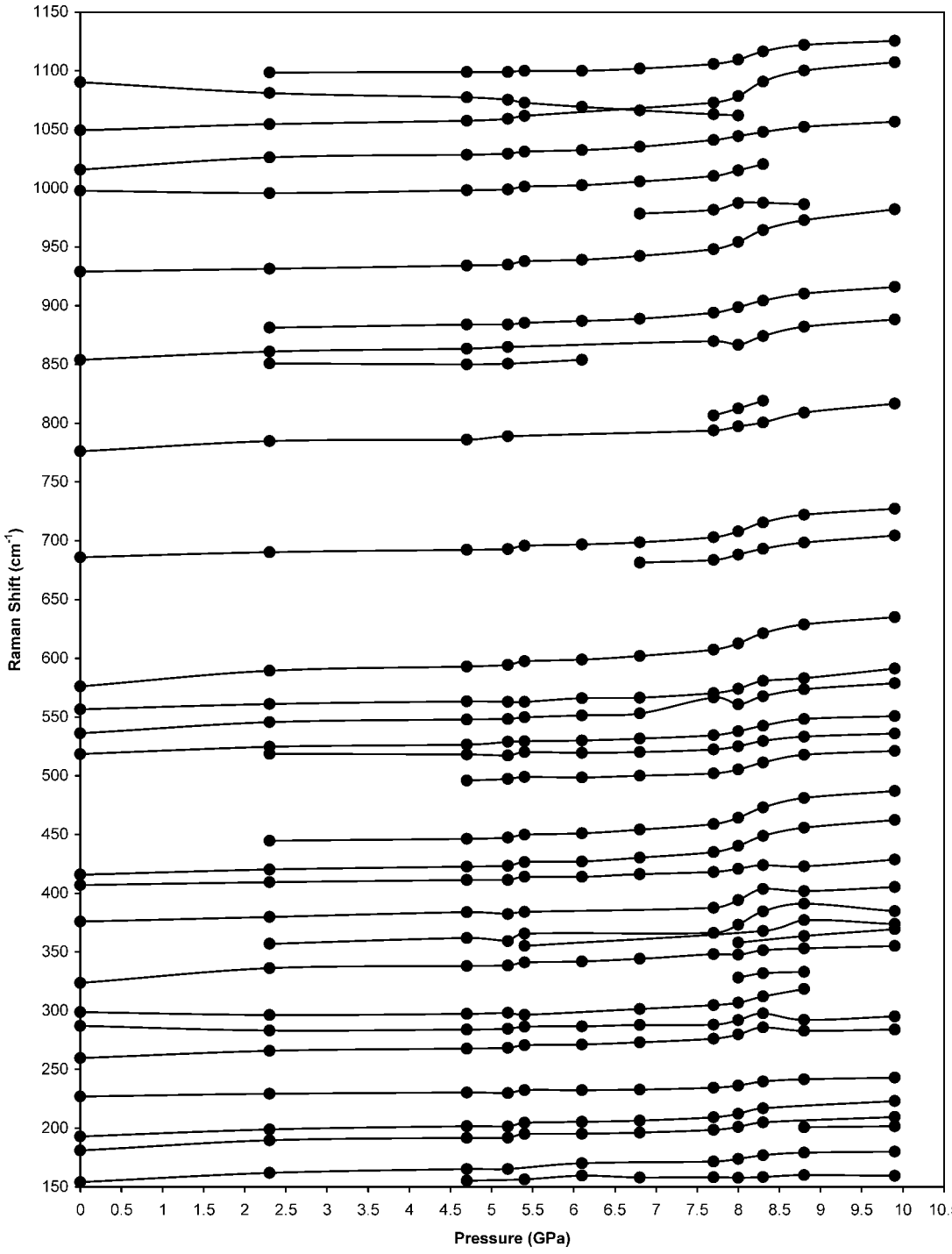

FIG. 4. Shift of Raman peaks with pressure. Note that the lines connecting data points are only visual guides to aid the reader. Also, note that there is a change in the slope of the lines near 8 GPa, which may be an indication of a change in the crystal structure. No X-ray data has yet been collected on this material at these pressures.

observed, which supports the retention of the $P2_1/c$ phase but is in contrast to the changes observed in the Raman spectra. In both kosmochlor and Li-kosmochlor pyroxene samples, the absorption profile shows a continuous hypsochromic shift of the maximum absorption of visible light with increasing pressure (Fig. 5). The decrease in absorption maxima with increasing pressure reflects the increase in energy of the bonds and concurrent increase in ligand field energy that results from shortening due to decrease in cell volume. Shorter bonds equate to an increase in electron density between the atoms and a corresponding increase in the energy of the bond, reflected by the decrease in wavelengths absorbed by the sample. Interestingly, the data from $NaCrSi_2O_6$ indicates that the ligand field surrounding the chromium atom is weaker than in $LiCrSi_2O_6$: the centers of maximum absorption for the $NaCrSi_2O_6$ appear at longer wavelengths than the centers for $LiCrSi_2O_6$. This is counterintuitive, as one might think that the size of the Na^+ ion is larger, so the ligand field surrounding the chromium ion would be more energetic due to the close proximity of the atoms; however, it is consistent with the

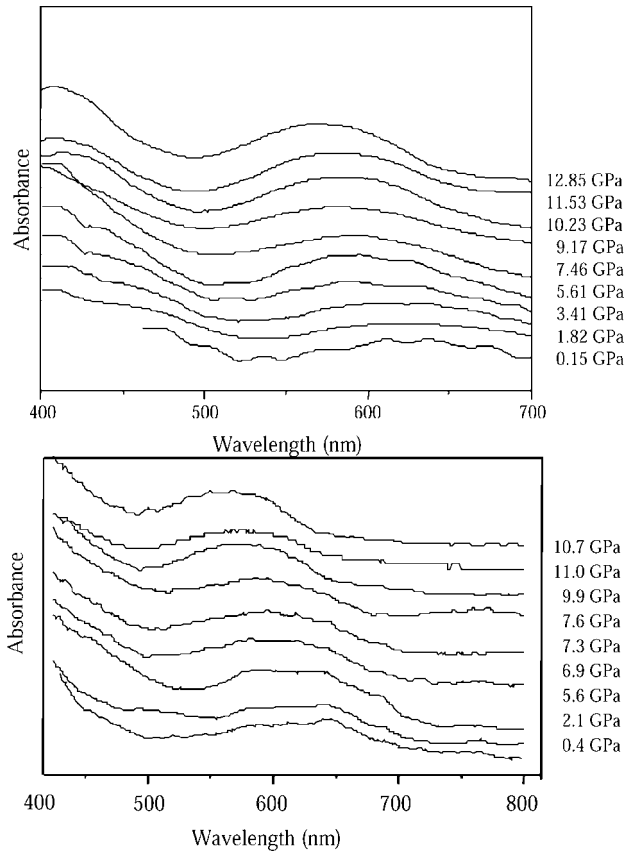

FIG. 5. Visible absorption spectra of (**top**) $NaCrSi_2O_6$ and (**bottom**) $LiCrSi_2O_6$. The error in pressure measurements is estimated at (**top**) 0.05 GPa and (**bottom**) 0.1 GPa. The increased error in the bottom spectra is due to deviatoric stress applied to the ruby. The plots demonstrate that the energy of the light absorbed increases with pressure.

observation from crystal structure determination that the average Cr–O bond is somewhat shorter, and thus more energetic, for the LiCr phase ($<R(Cr–O)> = 1.99$ Å) than for the NaCr phase ($<R(Cr–O)> = 2.00$ Å).[6,14]

CONCLUSION

The vibrational spectra of $LiCrSi_2O_6$ were compared to the Raman spectra of $LiFeSi_2O_6$ and $LiAlSi_2O_6$. The extension of knowledge gained in the studies of spodumene and Li-acmite through Raman spectroscopy and single crystal X-ray crystallography enabled tentative assignment of some of the Raman modes of $LiCrSi_2O_6$ to specific atomic interactions. Additionally, the fact that these pyroxenes all contained 5-coordinated Li in the $P2_1/c$ phase and had similar spectra suggests that other Li-pyroxenes, such as $LiGaSi_2O_6$ and $LiVSi_2O_6$, may also display similar spectra and those spectra may also be able to be interpreted by comparison of the data contained herein. Study of the Raman spectra of the above two compounds will give additional information concerning the bonding of the Li-pyroxenes.

This study illustrated that the region near 700 cm^{-1}, which has been utilized as a benchmark for the $P2_1/c$ phase in pyroxenes, displays only a single peak in the $P2_1/c$ phase at low pressures, but at higher pressures displays a low-intensity second peak. This behavior is contrary to the use of a doublet in this region to indicate the $P2_1/c$ phase in pyroxenes, as this material is in the $P2_1/c$ phase throughout all pressures studied. Additionally, this Li-pyroxene, like the other two studied, displays a secondary change in the Raman spectrum at high pressure. It would be interesting to determine whether the doublet would appear in the Raman spectrum of a Li-pyroxene (such as $LiScSi_2O_6$) that displays a second-order (continuous) rather than a first-order (discontinuous) phase transition.[7,15]

Finally, the application of pressure to the sample increases the ligand field energy surrounding the M1 atom, which is illustrated by the decrease in wavelength of maximum visible light absorption. This behavior is commensurate with the behavior of $NaCrSi_2O_6$ under pressure, which does not display bonding changes at higher pressures, but does show a shift in the visible absorption spectrum with pressure.[11] There is no discontinuous color change that might indicate a phase transition of $LiCrSi_2O_6$.

The combination of the UV-visible data with the Raman spectra of the pyroxenes studied herein gives a more complete picture of the atomic-level changes occurring in Li-pyroxenes than has previously been available. While data on other pyroxenes should be collected, trends presented herein display important facts that may be generalized to other pyroxenes. Specifically, there is an increase in ligand field energy as crystal volume is decreased and atoms are brought closer together as pressure is increased. At pressures higher than the phase transition, a change in the Raman spectra is observed in all three pyroxenes studied herein. This change may be indicative of the first step towards a transition back to $C2/c$ symmetry and is expected to occur in other pyroxenes in $P2_1/c$ phase.

1. S. Maaloe and K. Aoki, Contrib. Mineral. Petrol. **63,** 161 (1977).
2. R. T. Downs, Am. Mineral. **88,** 556 (2003).
3. J. Revenaugh and T. H. Jordan, J. Geophys. Res. **96,** 19781 (1991).
4. A. B. Woodland, Geophys. Res. Lett. **25,** 1241 (1998).
5. R. T. Downs, G. V. Gibbs, and J. M. B. Boisen, EOS Transactions, AGU Fall Meeting Supplement 80, **46,** F1140 (1999).
6. G. J. Redhammer and G. Roth, Z. Kristallogr. **219,** 278 (2004).
7. G. J. Redhammer and G. Roth, Z. Kristallogr. **219,** 585 (2004).
8. G. J. Redhammer, G. Roth, W. Paulus, G. Andre, W. Lottermoser, G. Amthauer, W. Treutmann, and B. Koppelhuber-Bitschnau, Phys. Chem. Miner. **28,** 337 (2001).
9. C. J. S. Pommier, M. B. Denton, and R. T. Downs, J. Raman Spectrosc. **34,** 769 (2003).
10. C. J. S. Pommier, R. T. Downs, M. Stimpfl, G. J. Redhammer, and M. B. Denton, J. Raman Spectrosc. **36,** 864 (2005).
11. M. J. Origlieri, R. T. Downs, R. M. Thompson, C. J. S. Pommier, M. B. Denton, and G. E. Harlowe, Am. Mineral. **88,** 1025 (2003).
12. I. Orgzall, B. Lorenz, P. K. Dorhout, P. M. VanCalcar, K. Brister, T. Sander, and H. D. Hochheimer, J. Phys. Chem. Solids **61,** 123 (2000).
13. M. J. Origlieri, R. T. Downs, R. M. Thompson, C. J. S. Pommier, M. B. Denton, and G. E. Harlow, Am. Mineral. **88,** 1632 (2003).
14. M. Cameron, S. Sueno, C. T. Prewitt, and J. J. Papike, Am. Mineral. **58,** 594 (1973).
15. T. Arlt and R. J. Angel, Phys. Chem. Miner. **27,** 719 (2000).